

Synthesis and Characterization of Methylammonium Borohydride

Kathryn R. Graham,^{*,†,‡} Mark E. Bowden,^{§,†} and Tim Kemmitt^{†,||}

[†]MacDiarmid Institute for Advanced Materials and Nanotechnology, P.O. Box 600, Wellington 6140, New Zealand, [‡]Victoria University of Wellington, P.O. Box 600, Wellington 6140, New Zealand, [§]Pacific Northwest National Laboratory, P.O. Box 999, Richland, Washington 99352, United States, and ^{||}Industrial Research, Ltd., P.O. Box 31-310, Lower Hutt, New Zealand

Received August 3, 2010

A new borohydride, $[\text{CH}_3\text{NH}_3]^+[\text{BH}_4]^-$, has been synthesized through the metathesis of CH_3NH_2 and NaBH_4 in methylamine. Room-temperature X-ray diffraction studies have shown that $[\text{CH}_3\text{NH}_3]^+[\text{BH}_4]^-$ adopts a tetragonal unit cell with considerable hydrogen mobility similar to that observed in NH_3BH_3 . The kinetics and thermodynamics of hydrogen release have been investigated and were found to follow a similar pathway to that of $[\text{NH}_4]^+[\text{BH}_4]^-$. Decomposition of $[\text{CH}_3\text{NH}_3]^+[\text{BH}_4]^-$ occurred slowly at room temperature and rapidly at ca. 40 °C to form $[\text{BH}_2(\text{CH}_3\text{NH}_2)_2]^+[\text{BH}_4]^-$, the methylated analogue of the diammoniate of diborane. The decomposition has been investigated by means of *in situ* X-ray diffraction and solid state ^{11}B NMR spectroscopy and occurred in the absence of any detectable intermediates to form crystalline $[\text{BH}_2(\text{CH}_3\text{NH}_2)_2]^+[\text{BH}_4]^-$. $[(\text{CH}_3)_2\text{NH}_2]^+[\text{BH}_4]^-$ and $[\text{BH}_2\{(\text{CH}_3)_2\text{NH}\}_2]^+[\text{BH}_4]^-$ have also been synthesized through analogous routes, indicating a more general applicability of the synthetic method.

Introduction

The safe and efficient storage of hydrogen is a major challenge for the adoption of a hydrogen-based economy. An ideal hydrogen storage material should reversibly supply hydrogen at temperatures around 50–150 °C at modest pressure. Many physical and chemical systems have been intensively studied, although a system which fulfills these criteria is yet to be discovered.

Boron–nitrogen–hydrogen compounds have received a lot of attention for use in chemical hydrogen storage.^{1–3} The protic amine-hydrogens and hydridic borane-hydrogens of these compounds allow for the occurrence of an extensive dihydrogen bonding network,^{4,5} which in turn influences hydrogen loss. Ammonia borane NH_3BH_3 ⁶ and ammonium borohydride $[\text{NH}_4]^+[\text{BH}_4]^-$ ⁷ have the potential to be practical hydrogen storage materials because of their large hydrogen

content of 19.6 and 24.5 wt %, respectively, and their low hydrogen desorption temperatures of 53–160 °C.

The dehydrogenation of $[\text{NH}_4]^+[\text{BH}_4]^-$ in the solid state proceeds via a multistep mechanism.⁷ $[\text{NH}_4]^+[\text{BH}_4]^-$ first decomposes at 53 °C, releasing one molar equivalent of hydrogen to form the diammoniate of diborane ($[\text{BH}_2(\text{NH}_3)_2]^+[\text{BH}_4]^-$, DADB), an ionic isomer of NH_3BH_3 which is a crucial precursor to hydrogen release.⁸ This DADB then releases a further two moles of hydrogen in two stages occurring at 85 and 130 °C.⁷

Further mechanistic details of hydrogen release from $[\text{NH}_4]^+[\text{BH}_4]^-$ have not been reported, and in particular the role of dihydrogen bonding has not been determined. More details are known about NH_3BH_3 , however, which releases two equivalents of hydrogen at ca. 100 and 150 °C in the solid state.⁹ This first equivalent is subject to a long induction period in which the dihydrogen bonding network is disrupted and forms a mobile phase of NH_3BH_3 .^{8,10} This is regarded as a crucial step in the formation of DADB and subsequent hydrogen release.

The observation that disrupting the dihydrogen bonding promoted hydrogen release prompted us to consider

*To whom correspondence should be addressed. E-mail: k.benge@irl.cri.nz.

(1) Hamilton, C. W.; Baker, R. T.; Staubitz, A.; Manners, I. *Chem. Soc. Rev.* **2009**, *38*, 279–293.

(2) Langmi, H. W.; McGrady, G. S. *Coord. Chem. Rev.* **2007**, *251*, 925–935.

(3) Umegaki, T.; Yan, J. M.; Zhang, X. B.; Shioyama, H.; Kuriyama, N.; Xu, Q. *Int. J. Hydrogen Energy* **2009**, *34*, 2303–2311.

(4) Richardson, T.; de Gala, S.; Crabtree, R. H.; Siegbahn, P. E. M. *J. Am. Chem. Soc.* **1995**, *117*, 12875–12876.

(5) Klooster, W. T.; Koetzle, T. F.; Siegbahn, P. E. M.; Richardson, T. B.; Crabtree, R. H. *J. Am. Chem. Soc.* **1999**, *121*, 6337–6343.

(6) Stephens, F. H.; Pons, V.; Baker, R. T. *Dalton Trans.* **2007**, 2613–2626.

(7) Karkamkar, A.; Kathmann, S. M.; Schenter, G. K.; Heldebrant, D. J.; Hess, N.; Gutowski, M.; Autrey, T. *Chem. Mater.* **2009**, *21*, 4356–4358.

(8) Stowe, A. C.; Shaw, W. J.; Linehan, J. C.; Schmid, B.; Autrey, T. *Phys. Chem. Chem. Phys.* **2007**, *9*, 1831–1836.

(9) Baitalow, F.; Baumann, J.; Wolf, G.; Jaenicke-Rossler, K.; Leitner, G. *Thermochim. Acta* **2002**, *391*, 159–168.

(10) Shaw, W. J.; Bowden, M.; Karkamkar, A.; Howard, C. J.; Heldebrant, D. J.; Hess, N. J.; Linehan, J. C.; Autrey, T. *Energy Environ. Sci.* **2010**, *3*, 796–804.

$[\text{NH}_4]^+[\text{BH}_4]^-$ derivatives, beginning with N-methyl substitution. The introduction of methyl groups is expected to disrupt the dihydrogen bonding network, and we note that methylamine borane has a lower activation energy for hydrogen release than NH_3BH_3 . In this paper, we report the first synthesis of the methylated derivative of $[\text{NH}_4]^+[\text{BH}_4]^-$, methylammonium borohydride $[\text{CH}_3\text{NH}_3]^+[\text{BH}_4]^-$, and describe its structure and thermal decomposition.

Experimental Section

All reactions were performed in an inert atmosphere using standard Schlenk line and glovebox techniques.

Materials. All chemicals used in this study were supplied by Sigma-Aldrich and were used as supplied.

Synthesis of Precursors. The methyl ammonium fluoride precursor was prepared by reacting potassium fluoride and methylamine hydrochloride in a 1:1 molar ratio in an excess of anhydrous methanol at room temperature. Complete reaction was achieved overnight.

Synthesis of Methylammonium Borohydride. In a typical reaction, methyl ammonium fluoride (0.02 mol) and sodium borohydride (0.01 mol) were loaded into an oven-dried, two-neck, 100 mL round-bottom flask containing a magnetic stir bar and fitted with a sintered glass filter. This flask was then cooled in a dry ice/acetone bath ($-78\text{ }^\circ\text{C}$), which was connected to a source of dry methylamine.

The methylamine generator used was a modification of that previously reported in the literature.¹² Once sufficient methylamine had been collected (*ca.* 40 mL), it was introduced into the cooled reaction flask. The resulting mixture was stirred for a minimum of 5 h under argon at $-78\text{ }^\circ\text{C}$. This reaction mixture was then filtered to remove any unreacted starting materials and insoluble byproduct. Methylamine was removed by evacuation, yielding a powdered white product. Yields were 70–75% on the basis of the quantity of NaBH_4 used. The products decomposed when dissolved in NMR solvents (THF, acetone, chloroform) and were instead characterized by solid-state NMR and X-ray powder diffraction as described in the Results and Discussion section.

Characterization of Materials. Powder X-ray diffraction utilized a Bruker D8 diffractometer fitted with $\text{Co K}\alpha$ radiation and parallel beam optics. Samples were loaded into a custom atmosphere protected cell inside the Ar drybox.

Crystallographic analysis was performed using TOPAS (Bruker AXS). Peak shapes derived from instrumental considerations¹³ were fitted to the observed patterns to optimize our proposed unit cells or crystal structures.

Solid-state ^{11}B NMR spectra were recorded at 11 T on a Bruker Avance 500 spectrometer without proton decoupling and referenced to $\text{BF}_3\cdot\text{Et}_2\text{O}$ (0 ppm). Samples were packed in silicon nitride rotors in the Ar glovebox and spun at *ca.* 10 kHz or greater at the magic angle in a Doty probe.

Thermal Decomposition. Thermal decomposition was conducted at a ramp rate of $1\text{ }^\circ\text{C}/\text{min}$ using a Pyrex flask on a temperature controlled hot plate. The composition of evolved gas was monitored using a quadrupole mass spectrometer (Dycor Dymaxion) with a flow (10 mL/min) of Ar carrier gas.

The quantity of gas evolved during decomposition was determined in separate experiments without a carrier gas by directing the outlet to a gas buret initially filled with paraffin oil.

Table 1. Final structural and agreement parameters for $[\text{CH}_3\text{NH}_3]^+[\text{BH}_4]^-$ ^a

atom	x	y	z
C	0	1/2	0.125(7)
HC1	-0.210	1/2	0.083
HC2	0.105	0.318	0.083
N	0	1/2	0.289(7)
HN1	0.200	1/2	0.329
HN2	-0.100	0.327	0.329
B	1/2	0	0.2984(6)
HB1	1/2	0	0.427
HB2	1/2	-0.219	0.255
HB3	0.310	0.110	0.255

^aTetragonal: space group $P4/nmm$ (No. 129). $a = 4.9486(3)$, $c = 8.9083(6)$ Å. B_{iso} for all atoms = $5.2(4)$ Å². Hydrogen positions constrained with occupancies described in the text. $R_{\text{wp}} = 12.09\%$, $R_{\text{exp}} = 6.61\%$, and $R_{\text{Bragg}} = 3.48\%$

Results and Discussion

Synthesis of $[\text{CH}_3\text{NH}_3]^+[\text{BH}_4]^-$. For our studies, we attempted to synthesize $[\text{CH}_3\text{NH}_3]^+[\text{BH}_4]^-$ from the metathesis of metal borohydrides MBH_4 and ammonium salts $\text{CH}_3\text{NH}_3\text{X}$ ($\text{M} = \text{Na}, \text{Li}, \text{K}$; $\text{X} = \text{Cl}, \text{F}$), in liquid methylamine.

The synthesis using NaBH_4 and LiBH_4 with $\text{CH}_3\text{-NH}_3\text{Cl}$ produced acceptable yields of 70–75% (based on MBH_4). However, the powder X-ray diffraction pattern of the isolated products showed crystalline peaks which corresponded to NaCl and LiCl . These salt by-products were present in the product irrespective of the ratio of reactants utilized, solvent concentration, or reaction time. While the presence of these Cl^- salts in the product is undesirable, the formation of NaCl or LiCl indicated a metathesis had occurred to form $[\text{CH}_3\text{-NH}_3]^+[\text{BH}_4]^-$. No reaction was observed when KBH_4 was used.

Due to the solubility of these chloride salts in methylamine, other methyl ammonium salts were considered. The synthesis of $[\text{NH}_4]^+[\text{BH}_4]^-$ from the metathesis reaction of NH_4F and MBH_4 in liquid ammonia has been reported,¹⁴ and on the basis of these results, the reaction was attempted using $\text{CH}_3\text{NH}_3\text{F}$. The solubility of NaF in CH_3NH_2 was found to be lower than that of NaCl , enabling complete removal from the reaction mixture by filtration.

The product isolated from the reaction between $\text{CH}_3\text{-NH}_3\text{F}$ and NaBH_4 is a white crystalline powder, free from NaF salt by X-ray diffraction. ^{11}B solid-state NMR showed only a single resonance at -37.9 ppm corresponding to BH_4^- . This chemical shift is lower than that expected for NaBH_4 (-41 ppm); therefore it can be concluded that no residual NaBH_4 was present in the isolated product.

The structure of $[\text{CH}_3\text{NH}_3]^+[\text{BH}_4]^-$ was determined using Rietveld analysis (see Table 1). A tetragonal unit cell with parameters $a = 4.9486$ and $c = 8.9083$ Å was identified using the trial and error indexing procedure of TOPAS. The volume of this cell appeared consistent with the expected density for $z = 2$ (calculated density = 0.71 g cm^{-3}), and the systematic absences were consistent with the primitive space groups $P4/n$ or $P4/nmm$. Atomic coordinates were determined by first refining rigid

(11) Bowden, M. E.; Brown, I. W. M.; Gainsford, G. J.; Wong, H. *Inorg. Chim. Acta* **2008**, *361*, 2147–2153.

(12) Mozingo, R.; McCracken, J. H. *Organic Syntheses* **1940**, *20*, 35–36.

(13) Cheary, R. W.; Coelho, A. J. *Appl. Crystallogr.* **1992**, *25*, 109–121.

(14) Heldebrant, D. J.; Karkamkar, A.; Linehan, J. C.; Autrey, T. *Energy Environ. Sci.* **2008**, *1*, 156–160.

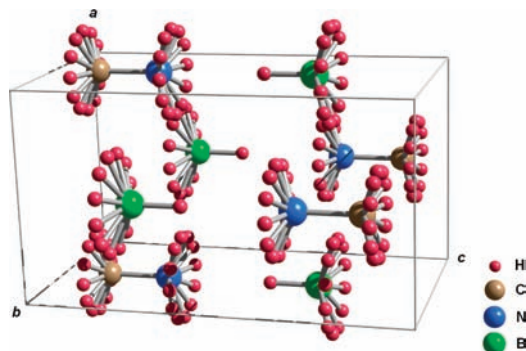


Figure 1. Room-temperature crystal structure of $[\text{CH}_3\text{NH}_3]^+[\text{BH}_4]^-$ as determined in this study. Twelve hydrogen atoms are positioned around each N and C atom, and 13 around each B to model rotational disorder. H, C, N, and B atoms are represented by red, brown, blue, and green, respectively.

CH_3NH_3 and BH_4 units in $P1$ with cell parameters constrained to their tetragonal values. The C, N, and B atoms all converged to positions very close to the 4-fold axes parallel to c in the tetragonal space groups; therefore, for the final refinements, they were positioned on these axes. As a result, the three hydrogen atoms bonded to C and to N are disordered over 12 positions encircling each atom (see Figure 1) in an identical manner to that of ammonia borane.^{15–17} Similarly, one of the BH_4^- hydrogen atoms converged to a position close to the 4-fold axis and was positioned on the axis to leave the remaining three disordered around the axis. This disorder has also been observed in methylammonium halides^{18,19} and indicated that rotation of the $-\text{CH}_3$ and $-\text{NH}_3$ groups occurred at ambient temperature. The halide structures have a similarly sized unit cell in $P4/nmm$, and therefore this space group was chosen for methylammonium borohydride.

Since X-rays are relatively insensitive to scattering from hydrogen, the hydrogen atoms were constrained in tetragonal coordination around C, N, and B with bond lengths typical for these elements. A significant improvement in the fit was observed when the occupancies of H bonded to B and N were adjusted to model the ionicity of methylammonium borohydride. A total of five hydrogens were distributed around B and two around N to provide the electron density expected in $[\text{CH}_3\text{NH}_3]^+[\text{BH}_4]^-$. This lowered the Bragg R factor from 7.96% to 3.48%, giving a final fit which confirms that the isolated product is methylammonium borohydride. The remaining minor discrepancies between observed and calculated diffraction patterns are most likely a result of constraints in the hydrogen positions. Further neutron experiments are in progress to determine hydrogen positions more precisely and to better characterize their disorder. Nevertheless, the

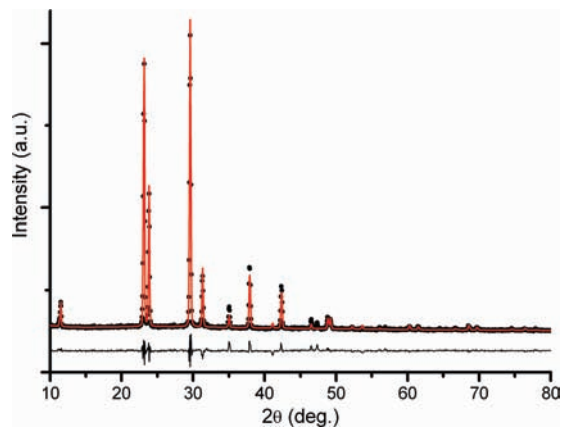


Figure 2. Calculated (solid line) and observed (points) X-ray diffraction traces of $[\text{CH}_3\text{NH}_3]^+[\text{BH}_4]^-$ with the difference shown below.

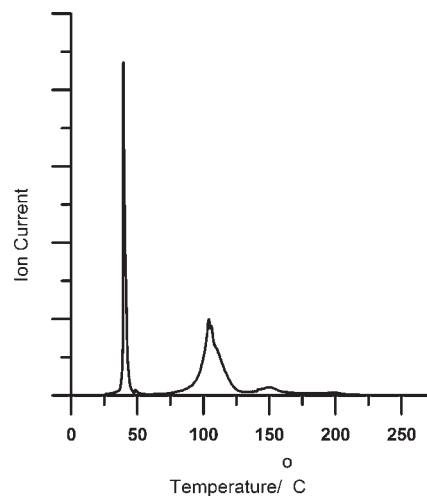


Figure 3. Hydrogen evolution from heating solid $[\text{CH}_3\text{NH}_3]^+[\text{BH}_4]^-$ at $1\text{ }^\circ\text{C}/\text{min}$, detected from mass spectrometry ($m/z\ 2$ signal).

$\text{H}\cdots\text{H}$ distances obtained in the present study indicate that methylammonium borohydride contains intermolecular dihydrogen bonds similar to those found in ammonia borane.^{4,15} The distance between the borohydride hydrogen positioned on the 4-fold axis and the ammonium hydrogens is 2.387 \AA , slightly less than the 2.4 \AA considered as the sum of van der Waals radii.⁵ The distance between the remaining borohydride hydrogens and the ammonium hydrogens is not able to be ascertained precisely because the rotational disorder of these atoms precludes establishing definite positions. However, the range of positions consistent with the molecular geometry gives a $\text{H}\cdots\text{H}$ distance between 1.63 and 2.24 \AA for the shortest interaction, further suggesting that intermolecular dihydrogen bonding is present.

The final refined coordinates are given in Table 1, and a plot showing the agreement between observed and calculated diffraction patterns is shown in Figure 2. A table of d spacings and intensities is provided in the Supporting Information.

Decomposition. Thermal Decomposition. Hydrogen is evolved upon heating solid $[\text{CH}_3\text{NH}_3]^+[\text{BH}_4]^-$. Evolved gas analysis by mass spectrometry recorded under increasing temperature (Figure 3) showed that three stages of hydrogen evolution occur up to $200\text{ }^\circ\text{C}$. Gas buret measurements show that 1 molar equivalent of hydrogen

(15) Hess, N. J.; Schenter, G. K.; Hartman, M. R.; Daemen, L. L.; Proffen, T.; Kathmann, S. M.; Mundy, C. J.; Hartl, M.; Heldebrant, D. J.; Stowe, A. C.; Autrey, T. *J. Phys. Chem. A* **2009**, *113*, 5723–5735.

(16) Yang, J. B.; Lamsal, J.; Cai, Q.; James, W. J.; Yelon, W. B. *Appl. Phys. Lett.* **2008**, *92*, 091916–3.

(17) Bowden, M. E.; Gainsford, G. J.; Robinson, W. T. *Aust. J. Chem.* **2007**, *60*, 149–153.

(18) Yamamuro, O.; Matsuo, T.; Suga, H.; David, W. I. F.; Ibberson, R. M.; Leadbetter, A. J. *Acta Crystallogr.* **1992**, *B48*, 329–336.

(19) Tsau, J.; Gilson, D. F. R. *Can. J. Chem.* **1970**, *48*, 717–722.

is released at *ca.* 40 °C, with a further two decomposition stages observed between 50 and 200 °C. Little is known about these higher-temperature events. However, during the second and third decomposition stages, large weight losses totaling *ca.* 45% were observed by thermogravimetric analysis, and large mass fragments were detected in the gas phase by means of mass spectrometry. The observation of these large mass fragments is consistent with the volatilization of a number of large cyclic methylborazanes. Crystals condensed on the cool part of the gas line were identified by X-ray diffraction as trimethylcyclotriborazane, similar to the behavior observed during the decomposition of $\text{CH}_3\text{NH}_2\text{BH}_3$.¹¹

The first stage of decomposition occurring at *ca.* 40 °C was further investigated and found to result in the formation of the methyl-substituted diammoniate of diborane, $[\text{BH}_2(\text{CH}_3\text{NH}_2)_2]^+[\text{BH}_4]^-$.²⁰ This compound was identified by XRD and solid-state ¹¹B NMR as described in a subsequent section. The decomposition reaction is analogous to that of simple $[\text{NH}_4]^+[\text{BH}_4]^-$, and therefore the same reaction pathway is expected:



The reaction enthalpy was measured using differential scanning calorimetry as -46 kJ/mol . This is similar to that reported for the decomposition of $[\text{NH}_4]^+[\text{BH}_4]^-$ (-40 kJ/mol)⁷ and provides further evidence that the two reactions proceed by a similar mechanism. The lower temperature observed for the decomposition of $[\text{CH}_3\text{NH}_3]^+[\text{BH}_4]^-$ compared to $[\text{NH}_4]^+[\text{BH}_4]^-$ indicates that steric hindrance does not slow the reaction but that the disruption of dihydrogen bonding introduced by the methyl group has resulted in a more facile reaction. This is consistent with the observation that amidoboranes, which have less dihydrogen bonding compared to ammonia borane, also release hydrogen at lower temperatures.^{21,22}

Room Temperature Decomposition. This first stage of decomposition also occurs slowly at room temperature, as observed for $[\text{NH}_4]^+[\text{BH}_4]^-$.^{7,23} Complete conversion of $[\text{CH}_3\text{NH}_3]^+[\text{BH}_4]^-$ to $[\text{BH}_2(\text{CH}_3\text{NH}_2)_2]^+[\text{BH}_4]^-$ at room temperature took place over *ca.* 72 h. This rate of hydrogen release was too slow to be reliably measured by our apparatus since we could not rule out the possibility of minor leaks or instabilities. $[\text{CH}_3\text{NH}_3]^+[\text{BH}_4]^-$ appears to have greater stability at room temperature than $[\text{NH}_4]^+[\text{BH}_4]^-$, which is reported to have a half-life of only 6 h at room temperature.²³ This is surprising given the lower temperature observed for decomposition of $[\text{CH}_3\text{NH}_3]^+[\text{BH}_4]^-$ under conditions of increasing temperature. However, it is consistent with the large temperature dependence of the release rate found for metal amidoboranes and methyl-substituted amidoboranes²² when

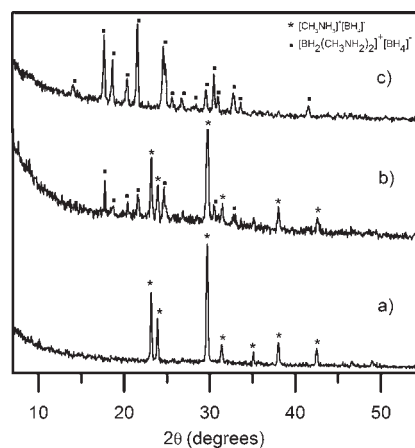


Figure 4. X-ray diffraction of the decomposition of $[\text{CH}_3\text{NH}_3]^+[\text{BH}_4]^-$ to $[\text{BH}_2(\text{CH}_3\text{NH}_2)_2]^+[\text{BH}_4]^-$. Pattern a was measured at a 0 mol hydrogen loss and shows crystalline peaks corresponding to $[\text{CH}_3\text{NH}_3]^+[\text{BH}_4]^-$ only (peaks marked with an asterisk). Pattern b was measured at a 0.5 mol hydrogen loss and shows peaks pertaining to both $[\text{CH}_3\text{NH}_3]^+[\text{BH}_4]^-$ and $[\text{BH}_2(\text{CH}_3\text{NH}_2)_2]^+[\text{BH}_4]^-$ (peaks marked by a dot). Pattern c was measured at a 1 mol hydrogen loss and shows peaks corresponding to $[\text{BH}_2(\text{CH}_3\text{NH}_2)_2]^+[\text{BH}_4]^-$ only.

compared to ammonia borane. Gas buret measurements coupled with X-ray diffraction studies (Figure 4) showed that full transition to $[\text{BH}_2(\text{CH}_3\text{NH}_2)_2]^+[\text{BH}_4]^-$ was achieved upon the loss of 1 mole of hydrogen, consistent with our proposed stoichiometries. The decomposition of $[\text{CH}_3\text{NH}_3]^+[\text{BH}_4]^-$ to $[\text{BH}_2(\text{CH}_3\text{NH}_2)_2]^+[\text{BH}_4]^-$ at room temperature is a solid to solid transition. *In situ* X-ray diffraction studies indicated that the conversion occurred without any visible crystalline intermediate phases (see the Supporting Information).

More detailed information about the chemical changes accompanying decomposition was sought using *in situ* solid-state ¹¹B NMR spectroscopy (Figure 5). It was not possible to accurately correlate the spectra with the amount of hydrogen loss or with sample temperature because of the additional heating imparted by the spinning rotor and RF power. Nevertheless, our results clearly showed that the BH_4 resonance of $[\text{CH}_3\text{NH}_3]^+[\text{BH}_4]^-$ (-37.9 ppm) decreased upon heating (and therefore hydrogen evolution) and was replaced by two new resonances at negative parts per million values of -38.4 ppm and -6.9 ppm corresponding respectively to the BH_4 and BH_2 sites of $[\text{BH}_2(\text{CH}_3\text{NH}_2)_2]^+[\text{BH}_4]^-$.

As discussed, $[\text{BH}_2(\text{CH}_3\text{NH}_2)_2]^+[\text{BH}_4]^-$ was isolated as a crystalline solid at room temperature. This is in agreement with previous studies²⁰ despite published reports of the existence of $[\text{BH}_2(\text{CH}_3\text{NH}_2)_2]^+[\text{BH}_4]^-$ as a nonvolatile liquid at room temperature.^{24,25} Identification of $[\text{BH}_2(\text{CH}_3\text{NH}_2)_2]^+[\text{BH}_4]^-$ was through ¹¹B NMR and powder X-ray diffraction. The original report of the powder diffraction pattern²⁰ lists only *d* spacings and relative intensities. We have been able to determine an orthorhombic unit cell for this compound ($a = 6.317 \text{ \AA}$, $b = 8.378 \text{ \AA}$, $c = 14.602 \text{ \AA}$) and a possible space group ($P2_12_12_1$, based on systematic absences). The volume of this cell gives a calculated density in agreement with

(20) Inoue, M.; Kodama, G. *Inorg. Chem.* **1968**, *7*, 430–433.

(21) Xiong, Z.; Yong, C. K.; Wu, G.; Chen, P.; Shaw, W.; Karkamkar, A.; Autrey, T.; Jones, M. O.; Johnson, S. R.; Edwards, P. P.; David, W. I. F. *Nat. Mater.* **2008**, *7*, 138–141.

(22) Luedtke, A. T.; Autrey, T. *Inorg. Chem.* **2010**, *49*, 3905–3910.

(23) Parry, R. W.; Schultz, D. R.; Girardot, P. R. *J. Am. Chem. Soc.* **1958**, *80*, 1–3.

(24) Beachley, O. T. *Inorg. Chem.* **1965**, *4*, 1823–1825.

(25) Shore, S. G.; Hickam, C. W.; Cowles, D. *J. Am. Chem. Soc.* **1965**, *87*, 2755–2756.

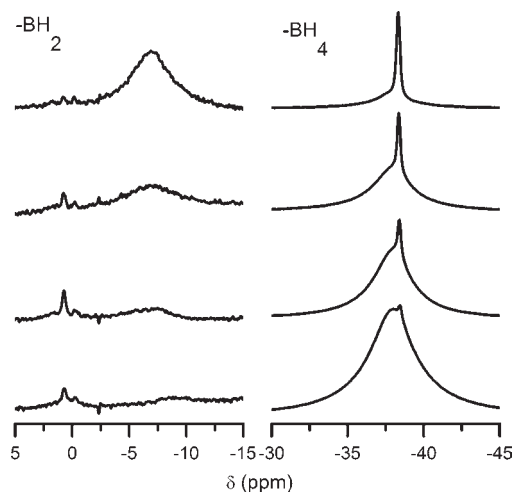


Figure 5. *In situ* solid-state ^{11}B NMR spectra showing the transformation of $[\text{CH}_3\text{NH}_3]^+[\text{BH}_4]^-$ to $[\text{BH}_2(\text{CH}_3\text{NH}_2)_2]^+[\text{BH}_4]^-$. The bearing gas temperatures ranged from $-10\text{ }^\circ\text{C}$ (bottom) to $40\text{ }^\circ\text{C}$ (top), although the sample temperature is expected to be higher owing to frictional and RF heating.

expectations (0.77 gcm^{-3} , $z = 4$), and the match with the experimental pattern is excellent. A plot of this match and an indexed table of d spacings and intensities are given in the Supporting Information.

Synthesis of Dimethylammonium Borohydride. The synthesis of dimethylammonium borohydride was also attempted using the method described. The product isolated from the reaction between $(\text{CH}_3)_2\text{NH}\cdot\text{HCl}$ and NaBH_4 in dimethylamine was a white crystalline powder, free from any impurities pertaining to starting materials utilized. Its diffraction trace did not match any patterns in the ICDD database, and NaCl was identified in the filtered solids, indicating that a metathesis had occurred to form $[(\text{CH}_3)_2\text{NH}_2]^+[\text{BH}_4]^-$. This product decomposed slowly at room temperature in a similar manner to $[\text{CH}_3\text{NH}_3]^+[\text{BH}_4]^-$ to yield a solid crystalline compound identified by its X-ray diffraction trace as the dimethyl derivative of the diammoniate of diborane $[\text{BH}_2\{(\text{CH}_3)_2\text{NH}\}_2]^+[\text{BH}_4]^-$.²⁰ The formation of this compound provided further evidence that we had been successful in synthesizing dimethylammonium borohydride.

Previous accounts in the literature have variously suggested that, at room temperature, $[\text{BH}_2\{(\text{CH}_3)_2\text{NH}\}_2]^+[\text{BH}_4]^-$ is an unstable liquid which evolves hydrogen,²⁵ or that it is a white solid that is stable *in vacuo*.²⁰ The latter work also reported that samples prepared from the metathesis of $[\text{BH}_2\{(\text{CH}_3)_2\text{NH}\}_2]^+\text{Cl}^-$ and NaBH_4 lost hydrogen slowly near $0\text{ }^\circ\text{C}$ to give a viscous liquid. Our results confirm that $[\text{BH}_2\{(\text{CH}_3)_2\text{NH}\}_2]^+[\text{BH}_4]^-$ is a stable solid at room temperature and

indicate that contrary reports most likely result from the presence of small quantities of impurities as suggested by Inoue and Kodama.²⁰ Further, we have demonstrated that the metathesis reactions undertaken provide a more general synthetic procedure for the formation of substituted ammonium borohydrides and their corresponding $[\text{BH}_2(\text{NRR}'\text{R}'')]_2^+[\text{BH}_4]^-$ derivatives, which does not require the use of diborane.

Conclusions

Methylammonium borohydride $[\text{CH}_3\text{NH}_3]^+[\text{BH}_4]^-$ has been synthesized for the first time from the metathesis of $\text{CH}_3\text{NH}_3\text{X}$ and MBH_4 in methylamine and is a crystalline solid at room temperature. A structure determination using X-ray powder data shows considerable hydrogen mobility, similar to that observed in NH_3BH_3 , in the tetragonal unit cell with lattice parameters of $a = 4.9486\text{ \AA}$ and $b = 8.9083\text{ \AA}$.

Hydrogen is released from neat $[\text{CH}_3\text{NH}_3]^+[\text{BH}_4]^-$ when heated with a sharp peak observed in the EGA trace at *ca.* $40\text{ }^\circ\text{C}$. One mole of hydrogen is released during this event to form the methyl derivative of the diammoniate of diborane $[\text{BH}_2(\text{CH}_3\text{NH}_2)_2]^+[\text{BH}_4]^-$. The decomposition of $[\text{CH}_3\text{NH}_3]^+[\text{BH}_4]^-$ to $[\text{BH}_2(\text{CH}_3\text{NH}_2)_2]^+[\text{BH}_4]^-$ also occurs slowly at room temperature without any observed intermediates. The described method has also been shown to be successful in the synthesis of the dimethyl derivatives of these compounds and is likely to have more widespread applicability.

Acknowledgment. The authors gratefully acknowledge the contributions made from discussions with our International Partnership for the Hydrogen Economy collaborators, especially Drs. Tom Autrey (Pacific Northwest National Lab), Martin Owen Jones (University of Oxford), and Bill David (Rutherford-Appleton Lab). Funding for this work was kindly provided by the MacDiarmid Institute for Advanced Materials and Nanotechnology. A portion of the research was performed using EMSL, a national scientific user facility sponsored by the Department of Energy's Office of Biological and Environmental Research and located at Pacific Northwest National Laboratory.

Supporting Information Available: Tables of d spacings and intensities for $[\text{CH}_3\text{NH}_3]^+[\text{BH}_4]^-$ and $[\text{BH}_2(\text{CH}_3\text{NH}_2)_2]^+[\text{BH}_4]^-$; figures of *in situ* XRD measurements and unit cell fit to the $[\text{BH}_2(\text{CH}_3\text{NH}_2)_2]^+[\text{BH}_4]^-$ XRD pattern; TGA trace of the thermal decomposition of $\text{CH}_3\text{BH}_3\text{BH}_4$; X-ray powder pattern of the decomposition product from $(\text{CH}_3)_2\text{NH}_2\text{BH}_4$. This material is available free of charge via the Internet at <http://pubs.acs.org>.